

---

# Quantitative Treatment of Decoherence

**Leonid Fedichkin and Vladimir Privman**

Center for Quantum Device Technology, Department of Physics and  
Department of Electrical and Computer Engineering, Clarkson University,  
Potsdam, New York 13699-5721, USA

## Abstract

We review several approaches to define and quantify decoherence. We find that a measure based on a norm of deviation of the density matrix is appropriate for quantifying decoherence for quantum registers. For a semiconductor double quantum dot charge qubit, evaluation of this measure is presented. For a general class of decoherence processes, including those occurring in semiconductor qubits, we establish that this measure is additive: It scales linearly with the number of qubits in the quantum register.

## 1 Introduction

Decoherence [1, 2, 3, 4, 5, 6, 7, 8, 9, 10, 11, 12, 13, 14, 15, 16, 17, 18, 19] is an important physical phenomenon occurring inevitably in most experiments dealing with quantum objects. It is usually defined as a process whereby the physical system of interest interacts with environment or other larger system with complex structure and, because of this interaction, changes its evolution from unperturbed, coherent internal dynamics. In some sense, the information about the initial and subsequent states of system undergoing decoherence is leaking into the outer world: The system is no longer described by a wave function, but rather by the statistical density matrix [20, 21, 22, 23, 24]. The quantum wave function description only applies to the total system, including the environmental modes, which has much more degrees of freedom. Because of the importance of quantum coherence for quantum information processing [25, 26, 27, 28, 29, 30, 31, 32, 33, 34, 35, 36, 37, 38, 39, 40, 41, 42, 43, 44, 45, 46, 47, 48, 49, 50, 51, 52, 53, 54, 55, 56, 57, 58, 59, 60, 61, 62, 63, 64, 65, 66], quantitative characterization of decoherence has become an active research field with many open problems.

Since quantum information processing requires maintaining high level of coherence, emphasis has recently shifted from large-time system dynamics at

experimentally better studied coherence-decay time scales to almost perfectly coherent dynamics at much shorter times. Many quantum systems proposed as candidates for qubits (quantum bits) for practical realizations of quantum computing require quantitative evaluation of their coherence. In other words, a single measure characterizing decoherence is desirable for comparison of different qubit designs and their optimization. Besides the evaluation of single qubit performance one also has to analyze scaling of decoherence as the register size (the number of qubits involved) increases. Direct quantitative calculations of decoherence of even few-qubit quantum registers are not feasible. Therefore, a practical approach has been to explore quantitative single-parameter measures of decoherence [67], develop techniques to calculate such measures at least approximately for realistic one- and two-qubit systems [68, 69], and then establish scaling (additivity [70, 71]) for multi-qubit quantum systems.

In Section 2, we outline different approaches to define and quantify decoherence. We argue that a measure based on a properly defined norm of deviation of the density matrix is appropriate for quantifying decoherence in quantum registers. For a semiconductor double quantum dot qubit, evaluation of this measure is reviewed in Section 3. For a general class of decoherence processes, including those occurring in semiconductor qubits considered in Section 3, we argue, in Section 4, that this measure is additive. Thus, the level of quantum noise scales linearly with the number of qubits.

## 2 Measures of Decoherence

In this section, we consider briefly several approaches to quantifying the degree of decoherence due to interactions with environment. In Subsection 2.1, we discuss the approach based on the asymptotic relaxation time scales. The entropy and idempotency-defect measures are reviewed in Subsection 2.2. The fidelity measure of decoherence is considered in Subsection 2.3. In Subsection 2.4, we review our results on the operator norm measures of decoherence. Subsection 2.5 discusses an approach to eliminate the initial-state dependence of the decoherence measures.

### 2.1 Relaxation Time Scales

Decoherence of quantum systems is frequently characterized by the asymptotic rates at which they reach thermal equilibrium at temperature  $T$ . One of the reasons for focusing on relaxation rates is that large-time behavior is relatively easy to observe in ensemble experiments. Markovian approximation schemes typically yield exponential approach to the limiting values of the density matrix elements for large times [21, 22, 23]. For a two-state system, this defines the time scales  $T_1$  and  $T_2$ , associated, respectively, with the approach by the diagonal (thermalization) and off-diagonal (dephasing, decoherence) density-matrix elements to their limiting values. More generally, for

large times we approximate deviations from stationary values of diagonal and off-diagonal density matrix elements as

$$\rho_{kk}(t) - \rho_{kk}(\infty) \propto e^{-t/T_{kk}}, \quad (1)$$

$$\rho_{jk}(t) \propto e^{-t/T_{jk}} \quad (j \neq k). \quad (2)$$

The shortest time among  $T_{kk}$  is often identified as  $T_1$ . Similarly,  $T_2$  can be defined as the shortest time among  $T_{n \neq m}$ . These definitions yield the characteristic times of thermalization and decoherence (dephasing).

For systems candidate for quantum computing realizations, noise effects are commonly reduced by working at very low temperatures and making their structure features nanosize for strong quantization. Then for the decoherence and thermalization times we have,  $T_2 \ll T_1$ , e.g., [21]. Therefore, the decoherence time is a more crucial parameter for quantum computing considerations. The time scale  $T_2$  is compared to the “clock” times of quantum control, i.e., the quantum gate functions,  $T_g$ , in order to ensure the fault-tolerant error correction criterion  $T_g/T_2 \leq O(10^{-4})$ , e.g., [66].

The disadvantages of this type of analysis are that the exponential behavior of the density matrix elements in the energy basis is applicable only for large times, whereas for quantum computing applications, the short-time behavior is usually relevant [18]. Moreover, while the energy basis is natural for large times, the choice of the preferred basis is not obvious for short and intermediate times [18, 72]. Therefore, the time scales  $T_1$  and  $T_2$  have limited applicability in evaluating quantum computing scalability.

## 2.2 Quantum Entropy

An alternative approach is to calculate the entropy [20] of the system,

$$S(t) = -\text{Tr}(\rho \ln \rho), \quad (3)$$

or the idempotency defect, also termed the first order entropy [73, 74, 75],

$$s(t) = 1 - \text{Tr}(\rho^2). \quad (4)$$

Both expressions are basis independent, have a minimum at pure states and effectively describe the degree of the state’s “purity.” Any deviation from a pure state leads to the deviation from the minimal values, 0, for both measures,

$$S_{\text{pure state}}(t) = s_{\text{pure state}}(t) = 0. \quad (5)$$

## 2.3 Fidelity

Writing the total Hamiltonian as follows,

$$H = H_S + H_B + H_I, \quad (6)$$

where  $H_S$  is the term describing internal system dynamics,  $H_B$  governs the evolution of environment, and  $H_I$  describes system-environment interaction, let us now define the fidelity [76, 77],

$$F(t) = \text{Tr}_S [\rho_{\text{ideal}}(t) \rho(t)]. \quad (7)$$

Here the trace is over the system degrees of freedom, and  $\rho_{\text{ideal}}(t)$  represents the pure-state evolution of the system under  $H_S$  only, without interaction with the environment ( $H_I = 0$ ). In general, the Hamiltonian term  $H_S$  governing the system dynamics can be time dependent. For the sake of simplicity throughout this review we restrict our analysis by constant  $H_S$  since approximate evaluation of decoherence can be done for qubits controlled by constant Hamiltonian. In this case

$$\rho_{\text{ideal}}(t) = e^{-iH_S t} \rho(0) e^{iH_S t}. \quad (8)$$

More sophisticated scenarios with qubits evolving under time dependent  $H_S$  were considered in [78, 79, 80].

The fidelity provides a certain measure of decoherence in terms of the difference between the “real,” environmentally influenced,  $\rho(t)$ , evolution and the “free” evolution,  $\rho_{\text{ideal}}(t)$ . It will attain its maximal value, 1, only provided  $\rho(t) = \rho_{\text{ideal}}(t)$ . This property relies on the fact the  $\rho_{\text{ideal}}(t)$  remains a projection operator (pure state) for all times  $t \geq 0$ .

As an illustrative example consider a two-level system decaying from the excited to ground state, when there is no internal system dynamics,

$$\rho_{\text{ideal}}(t) = \begin{pmatrix} 0 & 0 \\ 0 & 1 \end{pmatrix}, \quad (9)$$

$$\rho(t) = \begin{pmatrix} 1 - e^{-\Gamma t} & 0 \\ 0 & e^{-\Gamma t} \end{pmatrix}, \quad (10)$$

and the fidelity is a monotonic function of time,

$$F(t) = e^{-\Gamma t}. \quad (11)$$

Note that the requirement that  $\rho_{\text{ideal}}(t)$  is a pure-state (projection operator), excludes, in particular, any  $T > 0$  thermalized state as the initial system state. For example, let us consider the application of the fidelity measure for the infinite-temperature initial state of our two level system. We have

$$\rho(0) = \rho_{\text{ideal}}(t) = \begin{pmatrix} 1/2 & 0 \\ 0 & 1/2 \end{pmatrix}, \quad (12)$$

which is not a projection operator. The spontaneous-decay density matrix is then

$$\rho(t) = \begin{pmatrix} 1 - (e^{-\Gamma t}/2) & 0 \\ 0 & e^{-\Gamma t}/2 \end{pmatrix}. \quad (13)$$

The fidelity remains constant

$$F(t) = 1/2, \quad (14)$$

and it does not provide any information of the time dependence of the decay process.

## 2.4 Norm of Deviation

In this subsection we consider the operator norms [81] that measure the deviation of the system from the ideal state, to quantify the degree of decoherence as proposed in [67]. Such measures do not require the initial density matrix to be pure-state. We define the deviation according to

$$\sigma(t) \equiv \rho(t) - \rho_{\text{ideal}}(t). \quad (15)$$

We can use, for instance, the eigenvalue norm,

$$\|\sigma\|_{\lambda} = \max_i |\lambda_i|, \quad (16)$$

or the trace norm,

$$\|\sigma\|_{\text{Tr}} = \sum_i |\lambda_i|, \quad (17)$$

etc., where  $\lambda_i$  are the eigenvalues of the deviation operator (15). A more precise definition of the eigenvalue norm for a linear operator,  $A$ , is [81]

$$\|A\| = \sup_{\varphi \neq 0} \left[ \frac{\langle \varphi | A^\dagger A | \varphi \rangle}{\langle \varphi | \varphi \rangle} \right]^{1/2}. \quad (18)$$

Since density operators are bounded, their norms, as well the norm of the deviation, can be always evaluated. Furthermore, since the density operators are Hermitian, this definition obviously reduces to the eigenvalue norm (16). We also note that  $\|A\| = 0$  implies that  $A = 0$ .

The calculation of these norms is sometimes simplified by the observation that  $\sigma(t)$  is traceless. Specifically, for two-level systems, we get

$$\|\sigma\|_{\lambda} = \sqrt{|\sigma_{00}|^2 + |\sigma_{01}|^2} = \frac{1}{2} \|\sigma\|_{\text{Tr}}. \quad (19)$$

For our example of the two-level system undergoing spontaneous decay, the norm is

$$\|\sigma\|_{\lambda} = 1 - e^{-\Gamma t}. \quad (20)$$

## 2.5 Arbitrary Initial States

The measures considered in the preceding subsections quantify decoherence of a system provided its initial state is given. However, this is not always the case. In quantum computing, it is impractical to keep track of all the possible initial states for each quantum register, that might be needed for implementing

a particular quantum algorithm. Furthermore, even the preparation of the initial state can introduce additional noise. Therefore, for evaluation of fault-tolerance (scalability), it will be necessary to obtain an upper-bound estimate of decoherence for an arbitrary initial state.

To characterize decoherence for an arbitrary initial state, pure or mixed, we proposed [67] to use the maximal norm,  $D$ , which is determined as an operator norm maximized over all initial density matrices. It is defined as the worst case scenario error,

$$D(t) = \sup_{\rho(0)} \left( \|\sigma(t, \rho(0))\|_{\lambda} \right). \quad (21)$$

For realistic two-level systems coupled to various types of environmental modes, the expressions of the maximal norm are surprisingly elegant and compact. They are usually monotonic and contain no oscillations due to the internal system dynamics, as, for example, are the results obtained for semiconductor quantum dot qubits considered in the next section.

In summary, we have considered several approaches to quantifying decoherence: relaxation times, entropy and fidelity measures, and norms of deviation, and we defined the maximal measure that is not dependent on the initial state, and which will be later shown to be additive; see Section 4.

### 3 Decoherence of Double Quantum Dot Charge Qubits

As a representative example, let us review evaluation of decoherence for semiconductor quantum dots. Quantum devices based on solid-state nanostructures have been among the major candidates for large-scale quantum computation because they can draw on existing advances in nanotechnology and materials processing [82]. Several designs of semiconductor quantum bits (qubits) were proposed [27, 28, 37, 41, 42, 43, 44, 83, 84, 85]. In particular, the encoding of quantum information into spatial degrees of freedom of electron placed in a quantum dot was considered in [41, 42, 43, 44, 85]. A relatively fast decay of coherence of electron states in ordinary quantum dots, e.g., [26], can be partially suppressed by encoding quantum information in a subspace of electron states in specially designed arrays of quantum dots (artificial crystals), proposed in [86]. Actually, under certain conditions even double-dot systems in semiconductors can be relatively well protected against decoherence due to their interactions with phonons and electromagnetic fields [38]. This observation was confirmed in recent experiments [45], which demonstrated coherent quantum oscillations of an electron in a double-dot structure.

Several designs of double-dot qubits have been explored in recent experiments [46, 47, 48, 49, 50] carried out at temperatures ranging from tens and hundreds of mK. Temperature dependence of relaxation rates in Si charge qubits was studied theoretically in [51, 52]. Recently, it has been pointed out [68] that in the zero-temperature limit and for conventional double-dot

structures higher order processes in electron-phonon interaction dominate decoherence.

In this work, we studied the acoustic phonon bath as the main source of decoherence for the considered type of qubit, which is supported by theoretical and experimental evidence, e.g., [38, 46]. Decoherence due to different sources, e.g., due to trapping center defects [87, 88], can play important role in other situations.

In the next subsection, we outline the structure of double-dot qubits. Subsections 3.2 and 3.3 are devoted to the consideration of the electron-phonon interaction for two realistic cases: In Subsection 3.2 we analyze the piezoacoustic interaction in crystals with zinc-blende lattice and with parabolic quantum dot confinement potential. Double-dots with prevalence of piezointeraction have been fabricated [45] in gated GaAs/AlGaAs heterostructures. In Subsection 3.3 we study the deformation interaction with acoustic phonons in “quantum dots” formed by double-impurities in semiconductors with inversion symmetry of elementary lattice cell. Experiments with the latter type of double-dot systems have been reported in [47, 48]. Finally, Subsections 3.4, 3.5, 3.6 and 3.7 present illustrative calculations of the noise level for selected quantum gates.

### 3.1 Model

We consider a double-dot structure sketched in Figure 1. It consists of two quantum dots coupled to each other via a tunneling barrier and containing a single electron hopping between the dots. We limit our consideration to double-dot structures in which the energy required to transfer to the upper levels is much higher than the lattice temperature and energy spacing between the two lowest levels.

The electron is considered to be in a superposition of two basis states,  $|0\rangle$  and  $|1\rangle$ ,

$$\psi = \alpha\psi_0 + \beta\psi_1. \quad (22)$$

The states that define the “logical” basis are not the physical ground and first excited state of the double-dot system. Instead,  $\psi_0$  (the “0” state of the qubit) is chosen to be localized at the first quantum dot and, to a zeroth order approximation, be similar to the ground state of that dot if it were isolated. Similarly,  $\psi_1$  (the “1” state) resembles the ground state of the second dot (if it were isolated). This assumes that the dots are sufficiently (but not necessarily exactly) symmetric. We denote the coordinates of the potential minima of the dots (dot centers) as vectors  $\mathbf{R}_0$  and  $\mathbf{R}_1$ , respectively. The distance between the dot centers is

$$L \equiv |\mathbf{L}| \equiv |\mathbf{R}_1 - \mathbf{R}_0|. \quad (23)$$

The Hamiltonian of an electron within a phonon environment is given by

$$H = H_e + H_p + H_{ep}. \quad (24)$$

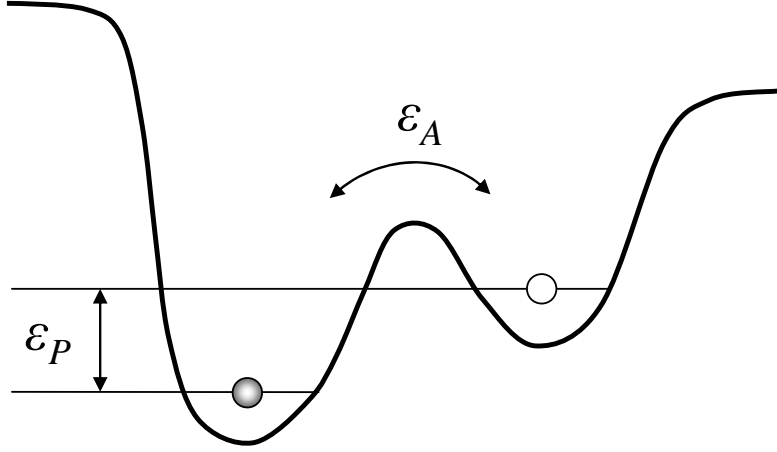


**Fig. 1.** Electron in a double well potential.

The electron term is

$$H_e = -\frac{1}{2}\varepsilon_A(t)\sigma_x - \frac{1}{2}\varepsilon_P(t)\sigma_z, \quad (25)$$

where  $\sigma_x$  and  $\sigma_z$  are Pauli matrices, whereas  $\varepsilon_A(t)$  and  $\varepsilon_P(t)$  can have time-dependent, as determined by unitary single-qubit quantum gate-functions that are carried out. They can be controlled externally by adjusting the potential on the control electrodes (gates) surrounding the double-dot system. For constant  $\varepsilon_A$  and  $\varepsilon_P$ , the energy splitting between the electron energy levels is

$$\varepsilon = \sqrt{\varepsilon_A^2 + \varepsilon_P^2}. \quad (26)$$

The Hamiltonian of the phonon bath is described by

$$H_p = \sum_{\mathbf{q},\lambda} \hbar\omega_q b_{\mathbf{q},\lambda}^\dagger b_{\mathbf{q},\lambda}, \quad (27)$$

where  $b_{\mathbf{q},\lambda}^\dagger$  and  $b_{\mathbf{q},\lambda}$  are, respectively, the creation and annihilation operators of phonons characterized by the wave vector  $\mathbf{q}$  and polarization  $\lambda$ . We approximately assume isotropic acoustic phonons, with a linear dispersion,

$$\omega_q = sq, \quad (28)$$

where  $s$  is the speed of sound in the semiconductor material. In the next subsection we show that the electron-phonon interaction can be derived in the form

$$H_{ep} = \sum_{\mathbf{q},\lambda} \sigma_z \left( g_{\mathbf{q},\lambda} b_{\mathbf{q},\lambda}^\dagger + g_{\mathbf{q},\lambda}^* b_{\mathbf{q},\lambda} \right), \quad (29)$$

with the coupling constants  $g_{\mathbf{q},\lambda}$  determined by the architecture of the double-dot and the properties of the material crystal structure.

### 3.2 Piezoelectric Interaction

The derivation in this subsection follows [68, 69]. The piezoacoustic electron-phonon interaction [89] is described by

$$H_{ep} = i \sum_{\mathbf{q},\lambda} \left( \frac{\hbar}{2\rho s q V} \right)^{1/2} M_{\lambda}(\mathbf{q}) F(\mathbf{q}) (b_{\mathbf{q}} + b_{-\mathbf{q}}^{\dagger}). \quad (30)$$

Here  $\rho$  is the density of the semiconductor material,  $V$  is the volume of semiconductor, and for the matrix element  $M_{\lambda}(\mathbf{q})$ , one can derive

$$M_{\lambda}(\mathbf{q}) = \frac{1}{2q^2} \sum_{ijk} (\xi_i q_j + \xi_j q_i) q_k M_{ijk}. \quad (31)$$

In this expression,  $\xi_j$  are the polarization vector components for polarization  $\lambda$ , while  $M_{ijk}$  express the electric field as a linear response to the stress,

$$E_k = \sum_{ij} M_{ijk} S_{ij}. \quad (32)$$

For a crystal with zinc-blende lattice, exemplified by GaAs, the tensor  $M_{ijk}$  has only those components non-zero for which all three indexes  $i, j, k$  are different; furthermore, all these components are equal  $M_{ijk} = M$ . Thus, we have

$$M_{\lambda}(\mathbf{q}) = \frac{M}{q^2} (\xi_1 q_2 q_3 + \xi_2 q_1 q_3 + \xi_3 q_1 q_2). \quad (33)$$

The form factor  $F(\mathbf{q})$  accounting for that the electrons in the quantum dot geometry are not plane waves, is

$$F(\mathbf{q}) = \sum_{j,k} c_j^{\dagger} c_k \int d^3 r \phi_j^*(\mathbf{r}) \phi_k(\mathbf{r}) e^{-i\mathbf{q} \cdot \mathbf{r}}, \quad (34)$$

where  $c_k, c_j^{\dagger}$  are annihilation and creation operators of the basis states  $k, j = 0, 1$ . For gate-engineered quantum dots, we consider the ground states in each dot to have an approximately Gaussian shape

$$\phi_j(\mathbf{r}) = \frac{1}{a^{3/2} \pi^{3/4}} e^{-|\mathbf{r} - \mathbf{R}_j|^2/2a^2}, \quad (35)$$

where  $2a$  is a characteristic size of the dots.

We assume that the distance between the dots,  $L$ , is sufficiently large compared to  $a$ , to ensure that the different dots wave functions do not overlap significantly,

$$\left| \int d^3 r \phi_j^*(\mathbf{r}) \phi_k(\mathbf{r}) e^{-i\mathbf{q} \cdot \mathbf{r}} \right| \ll 1, \quad \text{for } j \neq k. \quad (36)$$

This implies that the coupling leading to tunneling between the dots is small, as is the case for the recently studied experimental structures [45, 46, 47, 48], where the splitting due to tunneling, measured by  $\varepsilon_A$ , was below  $20 \mu\text{eV}$ , while the electron quantization energy in each dot was at least several meV.

For  $j = k$ , we obtain

$$\begin{aligned} \int d^3r \phi_j^*(\mathbf{r}) \phi_j(\mathbf{r}) e^{-i\mathbf{q}\cdot\mathbf{r}} &= \frac{1}{a^3 \pi^{3/2}} \int d^3r e^{-|\mathbf{r}-\mathbf{R}_j|^2/a^2} e^{-i\mathbf{q}\cdot\mathbf{r}} \\ &= e^{-i\mathbf{q}\cdot\mathbf{R}_j} e^{-a^2 q^2/4}. \end{aligned} \quad (37)$$

The resulting form factor is

$$F(q) = e^{-a^2 q^2/4} e^{-i\mathbf{q}\cdot\mathbf{R}} (c_0^\dagger c_0 e^{i\mathbf{q}\cdot\mathbf{L}/2} + c_1^\dagger c_1 e^{-i\mathbf{q}\cdot\mathbf{L}/2}), \quad (38)$$

where  $\mathbf{R} = (\mathbf{R}_0 + \mathbf{R}_1)/2$ . Finally, we get

$$F(q) = e^{-a^2 q^2/4} e^{-i\mathbf{q}\cdot\mathbf{R}} [\cos(\mathbf{q}\cdot\mathbf{L}/2) I + i \sin(\mathbf{q}\cdot\mathbf{L}/2) \sigma_z], \quad (39)$$

where  $I$  is the identity operator. Only the second term in (39), which is not proportional to  $I$ , represents an interaction affecting the qubit states. It leads to a Hamiltonian term of the form (29), with coupling constants

$$\begin{aligned} g_{\mathbf{q},\lambda} &= - \left( \frac{\hbar}{2\rho q s V} \right)^{1/2} M e^{-a^2 q^2/4 - i\mathbf{q}\cdot\mathbf{R}} \\ &\times (\xi_1 e_2 e_3 + \xi_2 e_1 e_3 + \xi_3 e_1 e_2) \sin(\mathbf{q}\cdot\mathbf{L}/2), \end{aligned} \quad (40)$$

where  $e_k = q_k/q$ .

### 3.3 Deformation Interaction

Deformation coupling with acoustic phonons [89] is described by

$$H_{ep} = \Xi \sum_{\mathbf{q},\lambda} \left( \frac{\hbar}{2\rho q s V} \right)^{1/2} q F(\mathbf{q}) (b_{\mathbf{q},\lambda}^\dagger + b_{-\mathbf{q},\lambda}), \quad (41)$$

where  $\Xi$  is a material-dependent constant termed the “deformation potential.”

Here we consider a particular double-dot-like nanostructure which has been a focus of recent experiments, due to advances in its fabrication [47, 48] by controlled single-ion implantation: A double-impurity Si structure with Hydrogen-like electron confinement potentials for at both impurities (P atoms). We consider a Hydrogen-like impurity state,

$$\phi_i(r) = \frac{1}{a^{3/2} \pi^{1/2}} e^{-|\mathbf{r}-\mathbf{R}_i|/a}, \quad (42)$$

where  $a$  is the effective Bohr radius. The form factor in this case is given by the following formula,

$$F(\mathbf{q}) = \frac{e^{-i\mathbf{q}\cdot\mathbf{R}}}{[1 + (a^2 q^2)/4]^2} [\cos(\mathbf{q}\cdot\mathbf{L}/2) I + i \sin(\mathbf{q}\cdot\mathbf{L}/2) \sigma_z]. \quad (43)$$

The interaction can then be expressed in the form (29), but with different coupling constants,

$$g_{\mathbf{q}} = i\Xi q \left( \frac{\hbar}{2\rho q s V} \right)^{1/2} \frac{e^{-i\mathbf{q} \cdot \mathbf{R}}}{[1 + (a^2 q^2)/4]^2} \sin(\mathbf{q} \cdot \mathbf{L}/2). \quad (44)$$

We note that the details of the electronic band structure, found important in recent decoherence studies [90] in other contexts, would matter for calculations that either consider decoherence due to processes mediated fully or partially by interactions of the bound electron with the conduction electrons, or if the impurity-bound electron were hybridized with the conduction electrons, namely if its wave function were affected by the lattice potential outside the dots. In our case, both effects are not considered. Specifically, we assume that the quantum dots are strongly binding and that the electron wave functions are approximately Gaussian or Hydrogen-like. While we do not expect the results to be modified significantly, consideration of the band structure effects could be an interesting future project especially for P-impurities in Si, where the bound-electron wave function actually extends well beyond the lattice spacing.

### 3.4 Error Estimates During Gate Functions

In general, the ideal qubit evolution governed by the Hamiltonian term (25) is time dependent. Decoherence estimates for some solid-state systems with certain shapes of time dependence of the system Hamiltonian were reported recently [78, 79, 80]. However, such calculations are rather complicated. Actually, there is no need to consider all possible time dependent controls of qubit to evaluate its performance. All single-qubit rotations which are required for quantum algorithms can be successfully implemented by using two constant-Hamiltonian gates, e.g., amplitude rotation and phase shift [64]. To perform both of these gates one can keep the Hamiltonian term (25) constant during the implementation of each gate, adjusting the parameters  $\varepsilon_A$  and  $\varepsilon_P$  as appropriate for each gate and for the idling qubit in between gate functions.

In the following subsections we give specific examples: In Subsection 3.5, we will consider decoherence during the implementation of the NOT gate (an amplitude gate). A  $\pi$ -phase shift gate is considered in Subsection 3.6. Then, in Subsection 3.7 we discuss the overall noise level estimate for a qubit subject to gate control.

### 3.5 Relaxation During the NOT Gate

The quantum NOT gate is a unitary operator which transforms the states  $|0\rangle$  and  $|1\rangle$  into each other. Any superposition of  $|0\rangle$  and  $|1\rangle$  transforms accordingly,

$$\text{NOT}(x|0\rangle + y|1\rangle) = y|0\rangle + x|1\rangle. \quad (45)$$

The NOT gate can be implemented by properly choosing  $\varepsilon_A$  and  $\varepsilon_P$  in the Hamiltonian term (25). Specifically, with constant

$$\varepsilon_A = \varepsilon \quad (46)$$

and

$$\varepsilon_P = 0, \quad (47)$$

the “ideal” NOT gate function is carried out, with these interaction parameters, over the time interval  $T_g = \tau$ ,

$$\tau = \frac{\pi\hbar}{\varepsilon}. \quad (48)$$

The dominant source of quantum noise for double-dot qubit subject to the NOT-gate type coupling, is relaxation involving energy exchange with the phonon bath (i.e., emission and absorption of phonons). In this case it is more convenient to study the evolution of the density matrix in the energy basis,  $\{|+\rangle, |-\rangle\}$ , where

$$|\pm\rangle = (|0\rangle \pm |1\rangle) / \sqrt{2}. \quad (49)$$

Then, assuming that the time interval of interest is  $[0, \tau]$ , the qubit density matrix can be expressed [22] as follows,

$$\rho(t) = \begin{pmatrix} \rho_{++}^{th} + [\rho_{++}(0) - \rho_{++}^{th}] e^{-\Gamma t} & \rho_{+-}(0) e^{-(\Gamma/2 - i\varepsilon/\hbar)t} \\ \rho_{-+}(0) e^{-(\Gamma/2 + i\varepsilon/\hbar)t} & \rho_{--}^{th} + [\rho_{--}(0) - \rho_{--}^{th}] e^{-\Gamma t} \end{pmatrix}. \quad (50)$$

This is the standard Markovian approximation for the evolution of the density matrix. For large times, this evolution would result in the thermal state, with the off-diagonal density matrix elements decaying to zero, while the diagonal ones approaching the thermal values proportional to the Boltzmann factors corresponding to the energies  $\pm\varepsilon/2$ . However, we are only interested in such evolution for a short time interval,  $\tau$ , of a NOT gate. The rate parameter  $\Gamma$  is the sum [22] of the phonon emission rate,  $W^e$ , and absorption rate,  $W^a$ ,

$$\Gamma = W^e + W^a. \quad (51)$$

The probability for the absorption of a phonon due to excitation from the ground state to the upper level is

$$w^\lambda = \frac{2\pi}{\hbar} |\langle f | H_{ep} | i \rangle|^2 \delta(\varepsilon - \hbar s q), \quad (52)$$

where  $|i\rangle$  is the initial state with the extra phonon with energy  $\hbar s q$  and  $|f\rangle$  is the final state,  $\mathbf{q}$  is the wave vector, and  $\lambda$  is the phonon polarization. Thus, we have to calculate

$$W^a = \sum_{\mathbf{q}, \lambda} w^\lambda = \frac{V}{(2\pi)^3} \sum_{\lambda} \int d^3 q w^\lambda. \quad (53)$$

For the interaction (29) one can derive

$$w^\lambda = \frac{2\pi}{\hbar} |g_{\mathbf{q},\lambda}|^2 N^{th} \delta(\varepsilon - \hbar s q), \quad (54)$$

where

$$N^{th} = \frac{1}{\exp(\hbar s q / k_B T) - 1} \quad (55)$$

is the phonon occupation number at temperature  $T$ , and  $k_B$  is the Boltzmann constant.

For the piezoacoustic interaction, the coupling constant in (40) depends on the polarization. For longitudinal phonons, the polarization vector has Cartesian components, expressed in terms of the spherical-coordinate angles,

$$\xi_1^\parallel = e_1 = \sin \theta \cos \phi, \quad \xi_2^\parallel = e_2 = \sin \theta \sin \phi, \quad \xi_3^\parallel = e_3 = \cos \theta, \quad (56)$$

where  $e_j = q_j/q$ . For transverse phonons, it is convenient to define the two polarization vectors  $\xi_i^{\perp 1}$  and  $\xi_i^{\perp 2}$  to have

$$\xi_1^{\perp 1} = \sin \phi, \quad \xi_2^{\perp 1} = -\cos \phi, \quad \xi_3^{\perp 1} = 0, \quad (57)$$

$$\xi_1^{\perp 2} = -\cos \theta \cos \phi, \quad \xi_2^{\perp 2} = -\cos \theta \sin \phi, \quad \xi_3^{\perp 2} = \sin \theta. \quad (58)$$

Then for longitudinal phonons, one obtains [69]

$$w^\parallel = \frac{\pi}{\rho s V q} M^2 e^{-a^2 q^2 / 4} \times 9 \sin^4 \theta \cos^2 \theta \sin^2 \phi \cos^2 \phi \sin^2(qL \cos \theta / 2). \quad (59)$$

For transverse phonons, one gets

$$w^{\perp 1} = \frac{\pi}{\rho s V q} M^2 e^{-a^2 q^2 / 4} (-2 \sin \theta \cos^2 \theta \sin \phi \cos \phi + \sin^3 \theta \cos \phi \sin \phi)^2 \sin^2(qL \cos \theta / 2), \quad (60)$$

$$w^{\perp 2} = \frac{\pi}{\rho s V q} M^2 e^{-a^2 q^2 / 4} (-2 \sin \theta \cos \theta \cos^2 \phi + \sin \theta \cos \theta \sin^2 \phi)^2 \sin^2(qL \cos \theta / 2). \quad (61)$$

By combining these contributions and substituting them in (53), we get the probability of absorption of a phonon for all polarizations,

$$W_{\text{piezo}}^a = \frac{M^2}{20\pi\rho s^2 \hbar L^5 k^4} \frac{\exp\left(-\frac{a^2 k^2}{2}\right)}{\exp\left(\frac{\hbar s k}{k_B T}\right) - 1} \times \left\{ (kL)^5 + 5kL \left[ 2(kL)^2 - 21 \right] \cos(kL) + 15 \left[ 7 - 3(kL)^2 \right] \sin(kL) \right\}, \quad (62)$$

where

$$k = \frac{\varepsilon}{\hbar s} \quad (63)$$

is the wave-vector of the absorbed phonon.

For the deformation interaction (44), one can obtain the following result,

$$w = \frac{\pi \Xi^2}{\rho s V} \frac{q}{[1 + (a^2 q^2)/4]^4} \sin^2(\mathbf{q} \cdot \mathbf{L}/2) \delta(\varepsilon - \hbar s q). \quad (64)$$

The total probability for a phonon absorption is

$$W_{\text{deform}}^a = \frac{\Xi^2}{4\pi\rho s^2 \hbar} \frac{k^3}{(1 + a^2 k^2/4)^4} \frac{1 - \sin(kL)/(kL)}{\exp\left(\frac{\hbar s k}{k_B T}\right) - 1}. \quad (65)$$

Finally, the expressions for the phonon emission rates,  $W^e$ , can be obtained by multiplying the above expressions, (62) and (65), by  $(N_{th} + 1)/N_{th}$ .

### 3.6 Dephasing During a Phase Gate

The  $\pi$  gate is a unitary operator which does not change the absolute values of the probability amplitudes of a qubit in the superposition of the  $|0\rangle$  and  $|1\rangle$  basis states. It changes the relative phase between the probability amplitudes. Specifically, any superposition of  $|0\rangle$  and  $|1\rangle$  transforms according to

$$I(x|0\rangle + y|1\rangle) = x|0\rangle - y|1\rangle. \quad (66)$$

Over a time interval  $\tau$ , the  $\pi$  gate can be carried out with constant interaction parameters,

$$\varepsilon_A = 0 \quad (67)$$

and

$$\varepsilon_P = \varepsilon = \frac{\pi \hbar}{\tau}. \quad (68)$$

In [68], double-dot qubit dynamics during implementation of phase gates was considered. The relaxation dynamics is suppressed during the  $\pi$  gate, because there is no tunneling between the dots. Quantum noise then results due to pure dephasing, i.e., via the decay of the off-diagonal qubit density matrix elements, while the diagonal density matrix elements remain constant. In the regime of pure dephasing, the qubit density matrix can be represented as [72, 91]

$$\rho(t) = \begin{pmatrix} \rho_{00}(0) & \rho_{01}(0)e^{-B^2(t)+i\varepsilon t/\hbar} \\ \rho_{10}(0)e^{-B^2(t)-i\varepsilon t/\hbar} & \rho_{11}(0) \end{pmatrix}, \quad (69)$$

with the spectral function,

$$\begin{aligned} B^2(t) &= \frac{8}{\hbar^2} \sum_{\mathbf{q}, \lambda} \frac{|g_{\mathbf{q}, \lambda}|^2}{\omega_q^2} \sin^2 \frac{\omega_q t}{2} \coth \frac{\hbar \omega_q}{2k_B T} \\ &= \frac{V}{\hbar^2 \pi^3} \int d^3 q \sum_{\lambda} \frac{|g_{\mathbf{q}, \lambda}|^2}{q^2 s^2} \sin^2 \frac{q s t}{2} \coth \frac{\hbar q s}{2k_B T}. \end{aligned} \quad (70)$$

For the piezoelectric interaction, the coupling constant  $g_{\mathbf{q},\lambda}$  was obtained in (40), and expression for the spectral function takes the form

$$\begin{aligned} B_{\text{piezo}}^2(t) &= \frac{M^2}{2\pi^3 \hbar \rho s^3} \int_0^\infty q^2 dq \int_0^\pi \sin \theta d\theta \int_0^{2\pi} d\varphi \\ &\times \sum_{\lambda} \frac{(\xi_1^\lambda e_2 e_3 + \xi_2^\lambda e_1 e_3 + \xi_3^\lambda e_1 e_2)^2}{q^3} \exp(-a^2 q^2/2) \\ &\times \sin^2(qL \cos \theta) \sin^2 \frac{qst}{2} \coth \frac{\hbar qs}{2k_B T}, \end{aligned} \quad (71)$$

c.f. (56)-(58). For the deformation interaction, we have the coupling constant (44), and the expression for the spectral function is given by

$$\begin{aligned} B_{\text{deform}}^2(t) &= \frac{\Xi^2}{\pi^2 \hbar \rho s^3} \int_0^\infty q^2 dq \int_0^\pi \sin \theta d\theta \\ &\times \frac{\sin^2(qL \cos \theta)}{q(1 + (a^2 q^2)/4)^4} \sin^2 \frac{qst}{2} \coth \frac{\hbar qs}{2k_B T}. \end{aligned} \quad (72)$$

### 3.7 Qubit Error Estimates

The qubit error measure,  $D$ , is obtained from the density matrix deviation from the “ideal” evolution by using the operator norm approach [67] reviewed in Subsection 2.5. After lengthy intermediate calculations one gets [68] relatively simple expressions for the error during the NOT gate,

$$D_{\text{NOT}} = \frac{1 - e^{-\Gamma\tau}}{1 + e^{-\varepsilon/k_B T}}, \quad (73)$$

and the  $\pi$  gate,

$$D_\pi = \frac{1}{2} \left[ 1 - e^{-B^2(\tau)} \right]. \quad (74)$$

**Table 1.** Qubit parameters

Parameter	GaAs double-dot qubit	Si double-impurity qubit
$\rho$ , kg/m <sup>3</sup>	$5.31 \times 10^3$	$2.33 \times 10^3$
$s$ , m/s	$5.14 \times 10^3$	$9.0 \times 10^3$
$\Xi$ , eV	3.3	—
$e_{14}$ , C/m <sup>2</sup>	—	0.16
$\kappa$	—	12.8
$M$ , eV/m	—	$ee_{14}/(\varepsilon_0 \kappa)$
$L$ , nm	50	50
$a$ , nm	25	3

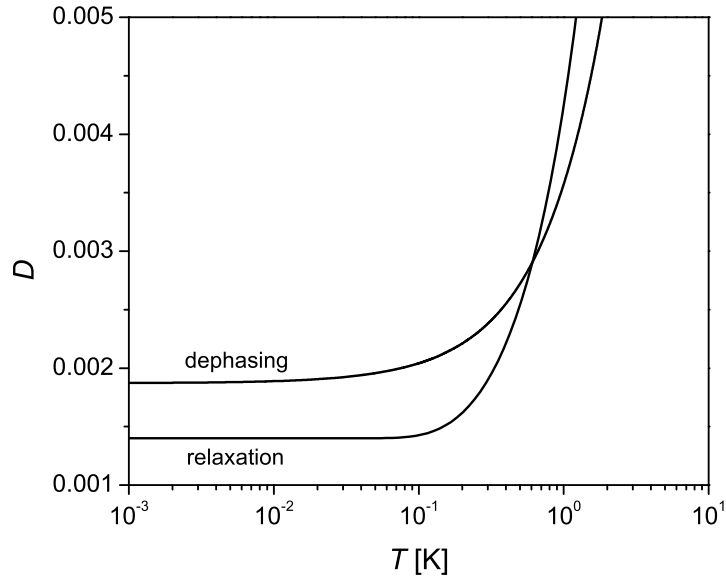


**Fig. 2.** Estimates of the error measure per cycle,  $D$ , due to the piezoelectric interaction in GaAs double-dot, shown as a function of the temperature,  $T$ . The cycle time  $\tau$  was  $6 \cdot 10^{-11}$  s.

A realistic noise estimate could be taken as the worst case scenario, i.e., the maximum of these two expressions for error per gate cycle. The expressions (73) and (74) were used to calculate the error rate for the double-dot qubit in GaAs and double-impurity qubit in Si. The parameters used were chosen to correspond to the experimentally realized structures, [46, 45, 47, 48], and are summarized in Table 1. The calculated error measures are presented in Figures 2 and 3. The gate time  $\tau$  selected for the reported calculations,  $6 \cdot 10^{-11}$  s, is a representative value consistent with typical experimental conditions. In fact, decreasing the gating time does not lead to smaller quantum noise in this case because the energy gap of the driven qubit is  $\sim 1/\tau$ . If the gap is made too large, other excitations will play a role in decoherence, for instance, optical phonons. The time scale chosen here is within an optimal range, as discussed in [68].

In summary, we derived expressions for the error measure for double-dot and double-impurity qubits. The results, presented in Figures 2 and 3, suggest that pure dephasing dominates at low temperatures. As the temperature increases beyond about 1 K, the effect of relaxation becomes comparable and ultimately dominant.

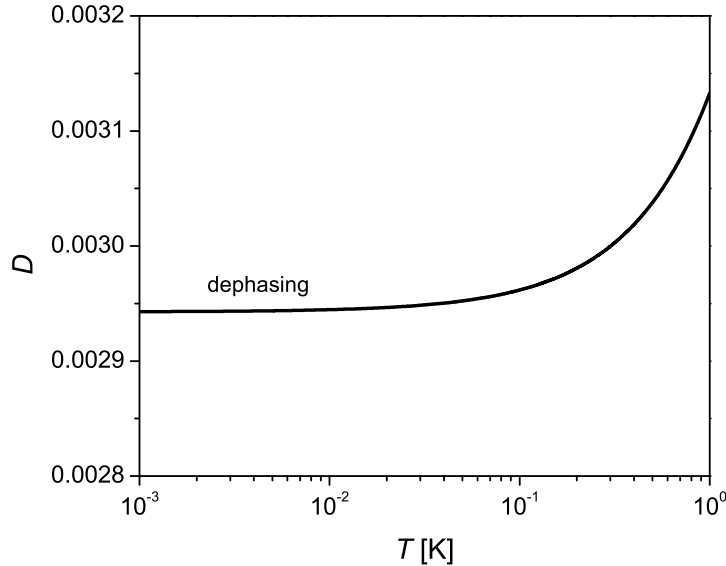


**Fig. 3.** Estimate of error rate per cycle,  $D$ , due to deformation phonon interaction for a double Phosphorus impurity in Si, shown as a function of the temperature,  $T$ . The cycle time  $\tau$  was  $6 \cdot 10^{-11}$  s. The relaxation rate for this range of the parameter values is negligibly small and respective values of  $D$  are not shown.

The error measure values found, are 1.5 or more orders of magnitude larger than the “traditional” fault-tolerance thresholds for multiqubit quantum computation, which range from  $O(10^{-4})$  down to  $O(10^{-6})$  [53, 54, 62, 65, 92, 93]. However, recent developments have yielded less strict requirements for the error rate [94, 95, 96], optimistically, as large as  $O(10^{-2})$ . Furthermore, there are several approaches to decrease decoherence effects by pulsed control [97, 98, 99, 100, 101, 102, 103, 104, 105, 106], some recently tested experimentally in multi-spin NMR [107, 108]. Other ideas rely on the fact that instead of the bulk material, the qubit could be manufactured in a one- or two-dimensional nanostructure [109, 110], the latter already available experimentally [111], which would affect the phonon spectrum and lower decoherence effects.

#### 4 Additivity of Decoherence Measures

In the study of decoherence of several-qubit systems, additional physical effects should be taken into account. Specifically, one has to consider the degree

to which noisy environments of different qubits are correlated [91, 112]. In addition to acting as a source of the quantum noise, the correlated bath can induce an effective interaction, namely, create entanglement, between the qubits immersed in it [110, 113, 114, 115]. Furthermore, if all constituent qubits are effectively immersed in the same bath, then there are ways to reduce decoherence for this group of qubits without error correction algorithms, by encoding the state of one logical qubit in a decoherence-free subspace of the states of several physical qubits [86, 91, 116, 117, 118]. In this section, we will consider several-qubit quantum registers and, as the “worst case scenario” assume that the qubits experience uncorrelated noise, i.e., each is coupled to a separate bath. Since analytical calculations for several qubits are not feasible, we seek “additivity” properties that will allow us to estimate the error measure for the register from the error measures of the constituent qubits.

It is important to emphasize that loss of quantum coherence results in a loss of various two- and several-qubit entanglements in the system. The highest order (multi-qubit) entanglements are “encoded” in the far off-diagonal elements of the multi-qubit register density matrix, and therefore these quantum correlations will decay at least as fast as the products of the decay factors for the qubits involved, as exemplified by several explicit calculations [119, 120, 121, 122]. This observation leads to the conclusion that, for large times, the *rates* of decay of coherence of the qubits will be additive.

However, here we seek a different result: one valid not in the regime of the asymptotic large-time decay of quantum coherence, but for relatively short times,  $\tau$ , of quantum gate functions, when the noise level, namely the value of the measure  $D(\tau)$  for each qubit, is relatively small. In this regime, we will establish [70] in this section, that, even for strongly entangled qubits—which is important for the utilization of the power of quantum computation—the error measures  $D$  of the individual qubits in a quantum register are additive. Thus, the error measure for a register made of similar qubits, scales up linearly with their number, consistent with other theoretical and experimental observations [76, 107, 108].

In Subsection 4.1, we revisit the noise measure via the maximal deviation norm and discuss some of its properties. In Subsection 4.2, we introduce the diamond norm which is used as an auxiliary tool in the proof of additivity. We then establish an approximate upper bound for  $D(t)$  for a register of several weakly interacting but possibly strongly entangled qubits, and cite work that further refines the additivity properties for typical qubit realizations.

#### 4.1 The Maximal Deviation Norm

To characterize decoherence for an arbitrary initial state, pure or mixed, we use the maximal norm,  $D$ , which was defined (21) in Subsection 2.5 as an operator norm maximized over all the possible initial density matrices. One can show that  $0 \leq D(t) \leq 1$ . This measure of decoherence will typically increase monotonically from zero at  $t = 0$ , saturating at large times at a value

$D(\infty) \leq 1$ . The definition of the maximal decoherence measure  $D(t)$  looks rather complicated for a general multiqubit system. However, it can be evaluated in closed form for short times, appropriate for quantum computing, for a single-qubit (two-state) system. We then establish an approximate additivity that allows us to estimate  $D(t)$  for several-qubit systems as well.

In the superoperator notation the evolution of the reduced density operator of the system (7) and the one for the ideal density matrix (8) can be formally expressed [62, 63, 64] in the following way

$$\rho(t) = T(t)\rho(0), \quad (75)$$

$$\rho^{(i)}(t) = T^{(i)}(t)\rho(0), \quad (76)$$

where  $T, T^{(i)}$  are linear superoperators. In this notation the deviation can be expressed as

$$\sigma(t) = [T(t) - T^{(i)}(t)]\rho(0). \quad (77)$$

The initial density matrix can always be written in the following form,

$$\rho(0) = \sum_j p_j |\psi_j\rangle\langle\psi_j|, \quad (78)$$

where  $\sum_j p_j = 1$  and  $0 \leq p_j \leq 1$ . Here the set of the wavefunctions  $|\psi_j\rangle$  is not assumed to have any orthogonality properties. Then, we get

$$\sigma(t, \rho(0)) = \sum_j p_j [T(t) - T^{(i)}(t)] |\psi_j\rangle\langle\psi_j|. \quad (79)$$

The deviation norm can thus be bounded,

$$\|\sigma(t, \rho(0))\|_\lambda \leq \left\| [T(t) - T^{(i)}(t)] |\phi\rangle\langle\phi| \right\|_\lambda. \quad (80)$$

Here  $|\phi\rangle$  is defined according to

$$\left\| [T - T^{(i)}] |\phi\rangle\langle\phi| \right\|_\lambda = \max_j \left\| [T - T^{(i)}] |\psi_j\rangle\langle\psi_j| \right\|_\lambda. \quad (81)$$

It transpires that for any initial density operator which is a statistical mixture, one can always find a density operator which is pure-state,  $|\phi\rangle\langle\phi|$ , such that  $\|\sigma(t, \rho(0))\|_\lambda \leq \|\sigma(t, |\phi\rangle\langle\phi|)\|_\lambda$ . Therefore, evaluation of the supremum over the initial density operators in order to find  $D(t)$ , see (21), can be done over only pure-state density operators,  $\rho(0)$ .

Let us consider strategies of evaluating  $D(t)$  for a single qubit. We can parameterize  $\rho(0)$  as

$$\rho(0) = U \begin{pmatrix} P & 0 \\ 0 & 1-P \end{pmatrix} U^\dagger, \quad (82)$$

where  $0 \leq P \leq 1$ , and  $U$  is an arbitrary  $2 \times 2$  unitary matrix,

$$U = \begin{pmatrix} e^{i(\alpha+\gamma)} \cos \theta & e^{i(\alpha-\gamma)} \sin \theta \\ -e^{i(\gamma-\alpha)} \sin \theta & e^{-i(\alpha+\gamma)} \cos \theta \end{pmatrix}. \quad (83)$$

Then, one should find a supremum of the norm of deviation (16) over all the possible real parameters  $P$ ,  $\alpha$ ,  $\gamma$  and  $\theta$ . As shown above, it suffices to consider the density operator in the form of a projector and put  $P = 1$ . Thus, one should search for the maximum over the remaining three real parameters  $\alpha$ ,  $\gamma$  and  $\theta$ .

Another parametrization of the pure-state density operators,  $\rho(0) = |\phi\rangle\langle\phi|$ , is to express an arbitrary wave function  $|\phi\rangle = \sum_j (a_j + ib_j)|j\rangle$  in some convenient orthonormal basis  $|j\rangle$ , where  $j = 1, \dots, N$ . For a two-level system,

$$\rho(0) = \begin{pmatrix} a_1^2 + b_1^2 & (a_1 + ib_1)(a_2 - ib_2) \\ (a_1 - ib_1)(a_2 + ib_2) & a_2^2 + b_2^2 \end{pmatrix}, \quad (84)$$

where the four real parameters  $a_{1,2}, b_{1,2}$  satisfy  $a_1^2 + b_1^2 + a_2^2 + b_2^2 = 1$ , so that the maximization is again over three independent real numbers. The final expressions (73) and (74) for  $D(t)$ , for our selected single-qubit systems considered in Section 3, are actually quite compact and tractable.

In quantum computing, the error rates can be significantly reduced by using several physical qubits to encode each logical qubit [86, 116, 117]. Therefore, even before active quantum error correction is incorporated [53, 54, 55, 56, 57, 58, 59, 60, 61], evaluation of decoherence of several qubits is an important, but formidable task. Thus, our aim is to prove the approximate additivity of  $D_q(t)$ , including the case of the initially strongly *entangled* qubits, labeled by  $q$ , whose dynamics is governed by

$$H = \sum_q H_q = \sum_q (H_{Sq} + H_{Bq} + H_{Iq}), \quad (85)$$

where  $H_{Sq}$  is the Hamiltonian of the  $q$ th qubit itself,  $H_{Bq}$  is the Hamiltonian of the environment of the  $q$ th qubit, and  $H_{Iq}$  is corresponding qubit-environment interaction. In the next subsection we consider a more complicated (for actual evaluation) diamond norm [62, 63, 64],  $K(t)$ , as an auxiliary quantity used to establish the additivity of the more easily calculable operator norm  $D(t)$ .

## 4.2 Upper Bound for Measure of Decoherence

The establishment of the upper-bound estimate for the maximal deviation norm of a multiqubit system, involves several steps. We derive a bound for this norm in terms of the recently introduced (in the context of quantum computing) [62, 63, 64] diamond norm,  $K(t)$ . Actually, for single qubits, in several models the diamond norm can be expressed via the corresponding maximal deviation norm. At the same time, the diamond norm for the whole quantum system is bounded by sum of the norms of the constituent qubits by using a specific stability property of the diamond norm. The use of the diamond norm was proposed in [62, 63, 64],

$$K(t) = \|T - T^{(i)}\|_{\diamond} = \sup_{\varrho} \|\{[T - T^{(i)}] \otimes I\} \varrho\|_{\text{Tr}}. \quad (86)$$

The superoperators  $T$ ,  $T^{(i)}$  characterize the actual and ideal evolutions according to (75), (76). Here  $I$  is the identity superoperator in a Hilbert space  $G$  whose dimension is the same as that of the corresponding space of the superoperators  $T$  and  $T^{(i)}$ , and  $\varrho$  is an arbitrary density operator in the product space of twice the number of qubits.

The diamond norm has an important stability property, proved in [62, 63, 64],

$$\|B_1 \otimes B_2\|_{\diamond} = \|B_1\|_{\diamond} \|B_2\|_{\diamond}. \quad (87)$$

Note that (87) is a property of the superoperators rather than that of the operators.

Consider a composite system consisting of the two subsystems  $S_1$ ,  $S_2$ , with the noninteracting Hamiltonian

$$H_{S_1 S_2} = H_{S_1} + H_{S_2}. \quad (88)$$

The evolution superoperator of the system will be

$$T_{S_1 S_2} = T_{S_1} \otimes T_{S_2}, \quad (89)$$

and the ideal one

$$T_{S_1 S_2}^{(i)} = T_{S_1}^{(i)} \otimes T_{S_2}^{(i)}. \quad (90)$$

The diamond measure for the system can be expressed as

$$\begin{aligned} K_{S_1 S_2} &= \|T_{S_1 S_2} - T_{S_1 S_2}^{(i)}\|_{\diamond} = \|(T_{S_1} - T_{S_1}^{(i)}) \otimes T_{S_2} + T_{S_1}^{(i)} \otimes (T_{S_2} - T_{S_2}^{(i)})\|_{\diamond} \\ &\leq \|(T_{S_1} - T_{S_1}^{(i)}) \otimes T_{S_2}\|_{\diamond} + \|T_{S_1}^{(i)} \otimes (T_{S_2} - T_{S_2}^{(i)})\|_{\diamond}. \end{aligned} \quad (91)$$

By using the stability property (87), we get

$$\begin{aligned} K_{S_1 S_2} &\leq \|(T_{S_1} - T_{S_1}^{(i)}) \otimes T_{S_2}\|_{\diamond} + \|T_{S_1}^{(i)} \otimes (T_{S_2} - T_{S_2}^{(i)})\|_{\diamond} = \\ &\quad \|T_{S_1} - T_{S_1}^{(i)}\|_{\diamond} \|T_{S_2}\|_{\diamond} + \|T_{S_1}^{(i)}\|_{\diamond} \|T_{S_2} - T_{S_2}^{(i)}\|_{\diamond} = \\ &\quad \|T_{S_1} - T_{S_1}^{(i)}\|_{\diamond} + \|T_{S_2} - T_{S_2}^{(i)}\|_{\diamond} = K_{S_1} + K_{S_2}. \end{aligned} \quad (92)$$

The inequality

$$K \leq \sum_q K_q, \quad (93)$$

for the diamond norm  $K(t)$  has thus been obtained. Let us emphasize that the subsystems can be initially entangled. This property is particularly useful for quantum computing, the power of which is based on qubit entanglement. However, even in the simplest case of the diamond norm of one qubit, the calculations are extremely cumbersome. Therefore, the use of the measure  $D(t)$  is preferable for actual calculations.

For short times, of quantum gate functions, we can use (93) as an approximate inequality for order of magnitude estimates of decoherence measures, even when the qubits are interacting. Indeed, for short times, the interaction

effects will not modify the quantities entering both sides significantly. The key point is that while the interaction effects are small, this inequality can be used for *strongly entangled* qubits.

The two deviation-operator norms considered are related by the following inequality

$$\|\sigma\|_\lambda \leq \frac{1}{2} \|\sigma\|_{\text{Tr}} \leq 1. \quad (94)$$

Here the left-hand side follows from

$$\text{Tr } \sigma = \sum_j \lambda_j = 0. \quad (95)$$

Therefore the  $\ell$ th eigenvalue of the deviation operator  $\sigma$  that has the maximum absolute value,  $\lambda_\ell = \lambda_{\max}$ , can be expressed as

$$\lambda_\ell = - \sum_{j \neq \ell} \lambda_j. \quad (96)$$

Thus, we have

$$\|\sigma\|_\lambda = \frac{1}{2} (2|\lambda_\ell|) \leq \frac{1}{2} \left( |\lambda_\ell| + \sum_{j \neq \ell} |\lambda_j| \right) = \frac{1}{2} \left( \sum_j |\lambda_j| \right) = \frac{1}{2} \|\sigma\|_{\text{Tr}}. \quad (97)$$

The right-hand side of (94) then also follows, because any density matrix has trace norm 1,

$$\|\sigma\|_{\text{Tr}} = \|\rho - \rho^{(i)}\|_{\text{Tr}} \leq \|\rho\|_{\text{Tr}} + \|\rho^{(i)}\|_{\text{Tr}} = 2. \quad (98)$$

From the relation (98) it follows that

$$K(t) \leq 2. \quad (99)$$

By taking the supremum of both sides of the relation (97) we get

$$D(t) = \sup_{\rho(0)} \|\sigma\|_\lambda \leq \frac{1}{2} \sup_{\rho(0)} \|\sigma\|_{\text{Tr}} \leq \frac{1}{2} K(t), \quad (100)$$

where the last step involves technical derivation details [70] not reproduced here. In fact, for a single qubit, calculations for typical models [70] give

$$D_q(t) = \frac{1}{2} K_q(t). \quad (101)$$

Since  $D$  is generally bounded by (or equal to)  $K/2$ , it follows that the multiqubit norm  $D$  is approximately bounded from above by the sum of the single-qubit norms even for the *initially entangled* qubits,

$$D(t) \leq \frac{1}{2} K(t) \leq \frac{1}{2} \sum_q K_q(t) = \sum_q D_q(t), \quad (102)$$

where  $q$  labels the qubits.

For specific models of decoherence of the type encountered in Section 3, as well as those formulated for general studies of short-time decoherence [67], a stronger property has been demonstrated [70], namely that the noise measures are actually equal, for low levels of noise,

$$D(t) = \sum_q D_q(t) + o\left(\sum_q D_q(t)\right). \quad (103)$$

In summary, in this section we considered the maximal operator norm suitable for evaluation of decoherence for a quantum register consisting of qubits immersed in noisy environments. We established the additivity property of this measure of decoherence for multi-qubit registers at short times, for which the level of quantum noise is low, and the qubit-qubit interaction effects are small, but without any limitation on the initial entanglement of the qubit register.

## Acknowledgments

We are grateful to A. Fedorov, D. Mozyrsky, D. Solenov and D. Tolkunov for collaborations and instructive discussions. This research was supported by the National Science Foundation, grant DMR-0121146.

## References

1. G. W. Ford, M. Kac and P. Mazur, *J. Math. Phys.* **6**, 504 (1965).
2. A. O. Caldeira and A. J. Leggett, *Physica A* **121**, 587 (1983).
3. S. Chakravarty and A. J. Leggett, *Phys. Rev. Lett.* **52**, 5 (1984).
4. H. Grabert, P. Schramm and G.-L. Ingold, *Phys. Rep.* **168**, 115 (1988).
5. N. G. van Kampen, *J. Stat. Phys.* **78**, 299 (1995).
6. K. M. Fonseca Romero and M. C. Nemes, *Phys. Lett. A* **235**, 432 (1997).
7. C. Anastopoulos and B. L. Hu, *Phys. Rev. A* **62**, 033821 (2000).
8. G. W. Ford and R. F. O'Connell, *Phys. Rev. D* **64**, 105020 (2001).
9. D. Braun, F. Haake and W. T. Strunz, *Phys. Rev. Lett.* **86**, 2913 (2001).
10. G. W. Ford, J. T. Lewis and R. F. O'Connell, *Phys. Rev. A* **64**, 032101 (2001).
11. J. Wang, H. E. Ruda and B. Qiao, *Phys. Lett. A* **294**, 6 (2002).
12. E. Lutz, *Phys. Rev. A* **67**, 022109 (2003).
13. A. Khaetskii, D. Loss and L. Glazman, *Phys. Rev. B* **67**, 195329 (2003).
14. R. F. O'Connell and J. Zuo, *Phys. Rev. A* **67**, 062107 (2003).
15. W. T. Strunz, F. Haake and D. Braun, *Phys. Rev. A* **67**, 022101 (2003).
16. W. T. Strunz and F. Haake, *Phys. Rev. A* **67**, 022102 (2003).
17. V. Privman, D. Mozyrsky and I. D. Vagner, *Comp. Phys. Commun.* **146**, 331 (2002).
18. V. Privman, *J. Stat. Phys.* **110**, 957 (2003).
19. V. Privman, *Mod. Phys. Lett. B* **16**, 459 (2002).
20. J. von Neumann, *Mathematical Foundations of Quantum Mechanics*, Princeton University Press, 1983.

21. A. Abragam, *The Principles of Nuclear Magnetism*, Clarendon Press, 1983.
22. K. Blum, *Density Matrix Theory and Applications*, Plenum, 1996.
23. N. G. van Kampen, *Stochastic Processes in Physics and Chemistry*, North-Holland, 1992.
24. W. H. Louisell, *Quantum Statistical Properties of Radiation*, Wiley, 1973.
25. A. Shnirman and G. Schön, in *Quantum Noise in Mesoscopic Physics*, Proc. NATO ARW *Quantum Noise in Mesoscopic Physics*, edited by Y. V. Nazarov, p. 357, Kluwer, 2003.
26. A. Ekert and R. Jozsa, *Rev. Mod. Phys.* **68**, 733 (1996).
27. V. Privman, I. D. Vagner and G. Kvetsel, *Phys. Lett. A* **239**, 141 (1998).
28. B. E. Kane, *Nature* **393**, 133 (1998).
29. D. Loss and D. P. DiVincenzo, *Phys. Rev. A* **57**, 120 (1998).
30. A. Imamoglu, D. D. Awschalom, G. Burkard, D. P. DiVincenzo, D. Loss, M. Sherwin and A. Small, *Phys. Rev. Lett.* **83**, 4204 (1999).
31. P. Zanardi and F. Rossi, *Phys. Rev. B* **59**, 8170 (1999).
32. Y. Nakamura, Y. A. Pashkin and H. S. Tsai, *Nature* **398**, 786 (1999).
33. T. Tanamoto, *Phys. Rev. A* **61**, 022305 (2000).
34. P. M. Platzman and M. I. Dykman, *Science* **284**, 1967 (1999).
35. G. P. Sanders, K. W. Kim, W. C. Holton, *Phys. Rev. A* **60**, 4146 (1999).
36. G. Burkard, D. Loss, D. P. DiVincenzo, *Phys. Rev. B* **59**, 2070 (1999).
37. R. Vrijen, E. Yablonovitch, K. Wang, H. W. Jiang, A. Balandin, V. Roychowdhury, T. Mor and D. P. DiVincenzo, *Phys. Rev. A* **62**, 012306 (2000).
38. L. Fedichkin, M. Yanchenko and K. A. Valiev, *Nanotechnology* **11**, 387 (2000).
39. S. Bandyopadhyay, *Phys. Rev. B* **61**, 13813 (2000).
40. A. A. Larionov, L. E. Fedichkin and K. A. Valiev, *Nanotechnology* **12**, 536 (2001).
41. J.A. Brum and P. Hawrylak, *Superlat. Microstr.* **22**, 431 (1997).
42. S. Bandyopadhyay, A. Balandin, V. P. Roychowdhury and F. Vatan, *Superlat. Microstr.* **23**, 445 (1998).
43. A. Balandin and K. L. Wang, *Superlat. Microstr.* **25**, 509 (1999).
44. L. A. Openov, *Phys. Rev. B* **60**, 8798 (1999).
45. T. Hayashi, T. Fujisawa, H.-D. Cheong, Y.-H. Jeong, Y. Hirayama, *Phys. Rev. Lett.* **91**, 226804 (2003).
46. T. Fujisawa, T. H. Oosterkamp, W. G. van der Wiel, B. W. Broer, R. Aguado, S. Tarucha and L. P. Kouwenhoven, *Science* **282**, 932 (1998).
47. L. C. L. Hollenberg, A. S. Dzurak, C. Wellard, A. R. Hamilton, D. J. Reilly, G. J. Milburn and R. G. Clark, *Phys. Rev. B* **69**, 113301 (2004).
48. T. M. Buehler, V. Chan, A. J. Ferguson, A. S. Dzurak, F. E. Hudson, D. J. Reilly, A. R. Hamilton, R. G. Clark, D. N. Jamieson, C. Yang, C. I. Pakes and S. Prawer, *Appl. Phys. Lett.* **88**, 192101 (2006).
49. P. A. Cain, H. Ahmed, D. A. Williams, *J. Appl. Phys.* **92**, 346 (2002).
50. C. G. Smith, S. Gardelis, J. Cooper, D. A. Ritchie, E. H. Linfield, Y. Jin and H. Launois, *Physica E* **12**, 830 (2002).
51. S. D. Barrett and G. J. Milburn, *Phys. Rev. B* **68**, 155307 (2003).
52. D. Ahn, *J. Appl. Phys.* **98**, 033709 (2005).
53. D. Aharonov and M. Ben-Or, e-print quant-ph/9611025 at [www.arxiv.org](http://www.arxiv.org) (1996).
54. D. Aharonov and M. Ben-Or, e-print quant-ph/9906129 at [www.arxiv.org](http://www.arxiv.org) (1999).

55. P. W. Shor, Phys. Rev. A **52**, 2493 (1995).
56. A. M. Steane, Phys. Rev. Lett. **77**, 793 (1996).
57. C. H. Bennett, G. Brassard, S. Popescu, B. Schumacher, J. A. Smolin and W. K. Wootters, Phys. Rev. Lett. **76**, 722 (1996).
58. A. R. Calderbank and P. W. Shor, Phys. Rev. A **54**, 1098 (1996).
59. A. M. Steane, Phys. Rev. A **54**, 4741 (1996).
60. D. Gottesman, Phys. Rev. A **54**, 1862 (1997).
61. E. Knill and R. Laflamme, Phys. Rev. A **55**, 900 (1997).
62. A. Y. Kitaev, Russ. Math. Surv. **52**, 1191 (1997).
63. D. Aharonov, A. Kitaev and N. Nisan, Proc. XXXth ACM Symp. Theor. Comp., Dallas, TX, USA, p. 20 (1998).
64. A. Y. Kitaev, A. H. Shen and M. N. Vyalyi, *Classical and Quantum Computation*, AMS, 2002.
65. J. Preskill, Proc. Roy. Soc. Lond. A **454**, 385 (1998).
66. D. P. DiVincenzo, Fort. Phys. **48**, 771 (2000).
67. L. Fedichkin, A. Fedorov and V. Privman, Proc. SPIE **5105**, 243 (2003).
68. L. Fedichkin and A. Fedorov, Phys. Rev. A **69**, 032311 (2004).
69. L. Fedichkin and A. Fedorov, IEEE Trans. Nanotech. **4**, 65 (2005).
70. L. Fedichkin, A. Fedorov and V. Privman, Phys. Lett. A **328**, 87 (2004).
71. A. Fedorov, L. Fedichkin and V. Privman, J. Comp. Theor. Nanoscience **1**, 132 (2004).
72. D. Mozyrsky and V. Privman, J. Stat. Phys. **91**, 787 (1998).
73. J. I. Kim, M. C. Nemes, A. F. R. de Toledo Piza and H. E. Borges, Phys. Rev. Lett. **77**, 207 (1996).
74. W. H. Zurek, Rev. Mod. Phys. **75**, 715 (2003).
75. J. C. Retamal and N. Zagury, Phys. Rev. A **63**, 032106 (2001).
76. B. J. Dalton, J. Mod. Opt. **50**, 951 (2003).
77. L.-M. Duan and G.-C. Guo, Phys. Rev. A **56**, 4466 (1997).
78. T. Brandes and T. Vorrath, Phys. Rev. B **66**, 075341 (2002).
79. T. Brandes, R. Aguado and G. Platero, Phys. Rev. B **69**, 205326 (2004).
80. D. Solenov and V. Privman, Int. J. Modern Phys. B **20**, 1476 (2006).
81. T. Kato, *Perturbation Theory for Linear Operators*, Springer-Verlag, 1995.
82. *Quantum Information Science and Technology Roadmap*, maintained online at [qist.lanl.gov](http://qist.lanl.gov).
83. D. Loss and D. P. DiVincenzo, Phys. Rev. A **57**, 120 (1998).
84. A. Imamoglu, D. D. Awschalom, G. Burkard, D. P. DiVincenzo, D. Loss, M. Sherwin and A. Small, Phys. Rev. Lett. **83**, 4204 (1999).
85. A. Barenco, D. Deutsch, A. Ekert and R. Jozsa, Phys. Rev. Lett. **74**, 4083 (1995).
86. P. Zanardi and M. Rasetti, Phys. Rev. Lett. **79**, 3306 (1997).
87. Y. Nakamura, Y. A. Pashkin, T. Yamamoto and J. S. Tsai, Phys. Rev. Lett. **88**, 047901 (2002).
88. I. Martin, D. Mozyrsky, and H. W. Jiang, Phys. Rev. Lett. **90**, 018301 (2003).
89. G. D. Mahan, *Many-Particle Physics*, Kluwer, 2000.
90. X. Hu, B. Koiller and S. Das Sarma, Phys. Rev. B **71**, 235332 (2005).
91. G. M. Palma, K. A. Suominen and A. K. Ekert, Proc. Roy. Soc. A **452**, 567 (1996).
92. E. Knill, R. Laflamme and W. H. Zurek, Proc. Roy. Soc. A **454**, 365 (1998).
93. P. Aliferis, D. Gottesman and J. Preskill, Quant. Inf. Comput. **6**, 97 (2006).

94. E. Knill, Phys. Rev. A **71**, 042322 (2005).
95. E. Knill, e-print quant-ph/0404104 at www.arxiv.org (2004).
96. E. Knill, Nature **434**, 39 (2005).
97. L. Viola, E. Knill and S. Lloyd, Phys. Rev. Lett. **82**, 2417 (1999).
98. L. Viola, S. Lloyd and E. Knill, Phys. Rev. Lett. **83**, 4888 (1999).
99. L. Fedichkin, Quant. Comp. Comput. **1**, 84 (2000).
100. M. S. Byrd and D. A. Lidar, Phys. Rev. Lett. **89**, 047901 (2002).
101. L. Viola, Phys. Rev. A **66**, 012307 (2002).
102. K. Khodjasteh and D. A. Lidar, Phys. Rev. A **68**, 022322 (2003).
103. Y. Ozhigov and L. Fedichkin, JETP Lett. **77**, 328 (2003).
104. L. Viola and E. Knill, Phys. Rev. Lett. **90**, 037901 (2003).
105. K. Khodjasteh and D. A. Lidar, Phys. Rev. Lett. **95**, 180501 (2005).
106. L. Viola and E. Knill, Phys. Rev. Lett. **94**, 060502 (2005).
107. H. G. Kojanski and D. Suter, Phys. Rev. Lett. **93**, 090501 (2004).
108. H. G. Kojanski and D. Suter, Phys. Rev. Lett. **97**, 150503 (2006).
109. M. I. Dykman and P. M. Platzman, Fortsch. Phys. **48**, 1095 (2000).
110. D. Solenov, D. Tolkunov and V. Privman, e-print cond-mat/0605278 at www.arxiv.org (2006).
111. M. M. Roberts, L. J. Klein, D. E. Savage, K. A. Slinker, M. Friesen, G. Celler, M. A. Eriksson and M. G. Lagally, Nature Materials **5**, 388 (2006).
112. A. Fedorov and L. Fedichkin, J. Phys. Cond. Mat. **18**, 3217 (2006).
113. D. Mozyrsky, A. Dementsov and V. Privman, Phys. Rev. B **72**, 233103 (2005).
114. D. Solenov, D. Tolkunov and V. Privman, Phys. Lett. A **359**, 81 (2006).
115. V. Privman, D. Solenov and D. Tolkunov, e-print quant-ph/0607076 at www.arxiv.org (2006).
116. L.-M. Duan and G.-C. Guo, Phys. Rev. Lett. **79**, 1953 (1997).
117. D. A. Lidar, I. L. Chuang and K. B. Whaley, Phys. Rev. Lett. **81**, 2594 (1998).
118. R. Doll, M. Wubs, P. Hänggi and S. Kohler, Europhys. Lett. **76**, 547 (2006).
119. T. Yu and J. H. Eberly, Phys. Rev. B **68**, 165322 (2003).
120. M. J. Storcz and F. K. Wilhelm, Phys. Rev. A **67**, 042319 (2003).
121. D. Tolkunov, V. Privman and P. K. Aravind, Phys. Rev. A **71**, 060308 (2005).
122. T. Yu and J. H. Eberly, Phys. Rev. Lett. **97**, 140403 (2006).